

Faithful and efficient hyperentanglement purification for spatial-polarization-time-bin photon system

Fang-Fang Du(杜芳芳), Gang Fan(樊钢), Yi-Ming Wu(吴一鸣), and Bao-Cang Ren(任宝藏)
Citation: Chin. Phys. B, 2023, 32 (**6**): 060304. DOI: 10.1088/1674-1056/aca395
Journal homepage: http://cpb.iphy.ac.cn; http://iopscience.iop.org/cpb

What follows is a list of articles you may be interested in

Complete hyperentangled Greenberger—Horne—Zeilinger state analysis for polarization and time-bin hyperentanglement

Zhi Zeng(曾志)
Chin. Phys. B, 2023, 32 (**6**): 060301. DOI: 10.1088/1674-1056/ac9044

Purification in entanglement distribution with deep quantum neural network

Jin Xu(徐瑾), Xiaoguang Chen(陈晓光), Rong Zhang(张蓉), and Hanwei Xiao(肖晗微)
Chin. Phys. B, 2022, 31 (**8**): 080304. DOI: 10.1088/1674-1056/ac6330

Short-wave infrared continuous-variable quantum key distribution over satellite-to-submarine channels

Qingquan Peng(彭清泉), Qin Liao(廖骎), Hai Zhong(钟海), Junkai Hu(胡峻凯), and Ying Guo(郭迎)
Chin. Phys. B, 2022, 31 (**6**): 060306. DOI: 10.1088/1674-1056/ac490a

Self-error-rejecting multipartite entanglement purification for electron systems assisted by quantum-dot spins in optical microcavities

Yong-Ting Liu(刘永婷), Yi-Ming Wu(吴一鸣), and Fang-Fang Du(杜芳芳)
Chin. Phys. B, 2022, 31 (**5**): 050303. DOI: 10.1088/1674-1056/ac4489

Low-overhead fault-tolerant error correction scheme based on quantum stabilizer codes

Xiu-Bo Chen(陈秀波), Li-Yun Zhao(赵立云), Gang Xu(徐刚), Xing-Bo Pan(潘兴博), Si-Yi Chen(陈思怡), Zhen-Wen Cheng(程振文), and Yi-Xian Yang(杨义先)
Chin. Phys. B, 2022, 31 (**4**): 040305. DOI: 10.1088/1674-1056/ac3817

Faithful and efficient hyperentanglement purification for spatial-polarization-time-bin photon system

Fang-Fang Du(杜芳芳)[1,†], Gang Fan(樊钢)[1], Yi-Ming Wu(吴一鸣)[1], and Bao-Cang Ren(任宝藏)[2,‡]

[1] *Science and Technology on Electronic Test and Measurement Laboratory, North University of China, Taiyuan* 030051, *China*
[2] *Department of Physics, Capital Normal University, Beijing* 100048, *China*

(Received 11 July 2022; revised manuscript received 17 October 2022; accepted manuscript online 17 November 2022)

We present a faithful and efficient hyperentanglement purification protocol (hyper-EPP) for nonlocal two-photon systems in spatial-polarization-time-bin hyperentangled Bell states. As the single-photon detectors can detect and herald the undesirable properties caused by side leakage and finite coupling strength, the parity-check gates and swap gates of our hyper-EPP in the spatial, polarization and time-bin mode degrees of freedom (DoFs) work faithfully. The qubit-flip errors in photon systems in three DoFs can be corrected effectively with the faithful parity-check gates and the photon pairs can be reused to distill high-fidelity ones by introducing the faithful swap gates, which greatly increases the efficiency of our hyper-EPP. Further, the maximal hyperentanglement can be obtained in principle by operating multiple rounds of the hyper-EPP.

Keywords: quantum communication, hyperentanglement purification, photon system, multiple degrees of freedom

PACS: 03.67.–a, 03.67.Hk, 03.67.Dd, 03.65.Ud **DOI:** 10.1088/1674-1056/aca395

1. Introduction

Quantum entanglement performs an important function in quantum information processing (QIP) and constitutes an essential resource for quantum communication and quantum computing. It has a wide range of applications in quantum key distribution,[1–6] quantum secret sharing,[7–12] quantum secure direct communication,[13–21] and so on. Nowadays, hyperentanglement, which refers to a quantum system that is simultaneously entangled in multiple degrees of freedom (DoFs) of photon systems,[22–26] has been demonstrated and has attracted widespread attention due to its excellent properties, including its high capacity, low loss rate, fewer quantum resources, and loss decoherence characteristics. For example, the time-bin DoF, i.e., two different times of arrival, is a stable DoF, as it only requires one path for transmission.[22] So far, hyperentanglement presents lots of unique opportunities for new kinds of QIP. For instance, it can be used to greatly improve the channel capacity and the security of quantum communication in linear photonic superdense coding,[26] entanglement witness,[27] quantum key distribution,[28] one-way quantum computing,[29] complete and deterministic Bell-state analysis, [30,31] teleportation-based quantum networking,[32] linear-optics heralded amplification,[33] hyperparallel quantum gates,[34–39] etc.

In practical long-distance QIP, the security and integrity of information will be affected by the quantum channel noise, as well as the distance and efficiency of transmission. In order to overcome the quantum channel noise problem, (hyper)entanglement purification provides us with a powerful way to regain the degraded mixed states into high-quality (hyper)entanglement states. Bennett *et al.*[40] presented the first entanglement purification protocol (EPP) for quantum systems, which expends some degraded entangled pairs to improve the purity of the remaining ones by performing local operations and classical communications (LOCC). Subsequently, entanglement purification has been well developed. Many important and practical recurrence EPPs,[41–55] deterministic EPPs,[56,57] and measurement-based EPPs[58–60] were proposed. For example, the recurrence EPPs have been well developed for linear polarization entanglement[41,42] and nonlinear optical systems,[43–45] atomic systems,[46] hyperentangled systems,[47–51] logic-qubit entangled systems,[52,53] nonlocal microwave photon systems,[54] d-level systems,[55] and so on. Recently, optical EPPs were designed.[61,62] EPP for optical and atomic systems has been demonstrated experimentally using linear optical elements.[63–65] Hu *et al.* proposed an efficient EPP with one polarization-spatial hyperentangled photon pair, where the efficiency of the EPP is 6600 times higher than that of the recurrence EPPs utilizing two pairs of low-fidelity entanglement.[66]

Generally, the parity-check gates can be used in the first step of the (hyper)EPPs to obtain the effective states of the final entanglement, and then the swap gates, which change the entanglement in a controllable way, will be used to improve the efficiency of (hyper)EPPs. The interaction between a single photon and a charged quantum dot (QD) in an optical mi-

†Corresponding author. E-mail: Duff@nuc.edu.cn
‡Corresponding author. E-mail: renbaocang@cnu.edu.cn

© 2023 Chinese Physical Society and IOP Publishing Ltd

crocavity can be used to construct parity-check gates (PCGs) and swap gates for hyperencoded photons. Under the imperfect scattering condition, i.e., the nonzero side leakage of the cavity and the finite coupling strength between the cavity and the QD, the fidelities and efficiencies of two kinds of gates will degrade drastically. However, a nonunity-fidelity parity-check gate will make some errors aimed at the orthogonal parity, and the imperfect swap gate will lead to an undesirable swapping process and change the state of the photons, which will inevitably cause secondary pollution to the original photon systems in the (hyper)EPP, and will limit the reliability of the (hyper)EPP. Therefore, it is of particular importance to construct the faithful (hyper)EPP with unity-fidelity parity-check and swap gates in practical scattering conditions.

In this paper, we present a faithful and efficient hyper-EPP for a nonlocal two-photon system in hyperentangled Bell states with bit-flip errors in the spatial, polarization, and time-bin mode DoFs assisted by QD-cavity systems. In the first step, we obtain information on the probability of each Bell state based on faithful PCGs in three DoFs. In the second step, we increase the probability of a useful Bell state in one or two DoFs by consuming some other two-photon systems based on faithful swap gates. The unity-fidelity PCG and swap gates are two key tools for implementing our hyper-EPP in a heralded way, as the errors coming from practical scattering are converted into the response of the detectors. Therefore, the bit-flip errors in three DoFs can be corrected effectively after several rounds of hyper-EPP. The maximal hyperentanglement in three DoFs, in principle, can be achieved.

2. Interactions between the photon and the QD in a single-sided microcavity

As the electronic spin confined in a charged semiconducting quantum dot (QD) has μs coherence time[67] and ps timescale single-qubit manipulation[68,69] easy to control and measure the spin state, and a QD embedded in an optical microcavity is the best platform for QD-spin QIP.[70] Many studies have improved the photon–electron–spin interactions by cascading the charged QDs coupled to nanophotonic micropillar cavities in experiments recently.[69,71,72] As shown in Fig. 1, a self-assembled In(Ga)As QD is embedded in the center of an optical resonant microcavity,[73] which can increase greatly the coupling strength of the QD-cavity. There are two distributed Bragg reflectors (DBRs) in the top and bottom of the microcavity respectively, and the bottom DBR is larger than the top DBR so that the bottom DBR has 100% reflectivity, while the top DBR has partial reflectivity. Injecting an extra electron into the QD can create a controlled negative exciton X^-, which comprises two electrons bound to one hole. Due to Pauli's exclusion principle, the spin-dependent optical transitions of the X^- are shown in Fig. 1. The electron-spin state $\uparrow$ ($\downarrow$) only interacts with left (right)-circularly polarized photon $|L\rangle$ ($|R\rangle$) to transition the state $|\uparrow\downarrow\Uparrow\rangle$ ($|\downarrow\uparrow\Downarrow\rangle$). Here $\uparrow$ ($\downarrow$) represents the spin state of the extra electron, and its projection on the z axis is $|+\frac{1}{2}\rangle$ ($|-\frac{1}{2}\rangle$). $|\uparrow\downarrow\Uparrow\rangle$ ($|\downarrow\uparrow\Downarrow\rangle$) represents the hole-spin state of the negative exciton (X^-), and its projection on the z axis is $|+\frac{3}{2}\rangle$ ($|-\frac{3}{2}\rangle$).

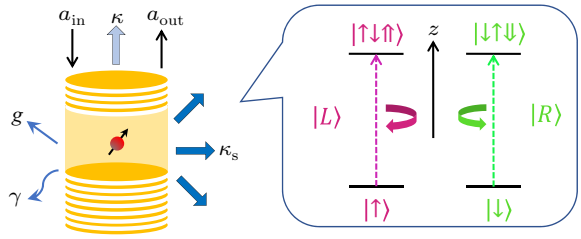


Fig. 1. Schematic diagram of the spin selection rule for optical transitions of the negatively charged exciton in a singly charged QD inside a single-sided optical microcavity.

The Heisenberg equations for the cavity field operator $\hat{a}$ and the QD dipole operator $\hat{\sigma}_-$ and $\hat{\sigma}_z$ are given by[73]

$$\begin{aligned}\frac{\mathrm{d}\hat{a}}{\mathrm{d}t} &= -\left[\mathrm{i}(\omega_{\rm c}-\omega)+\frac{\kappa}{2}+\frac{\kappa_{\rm s}}{2}\right]\hat{a}-g\hat{\sigma}_- -\sqrt{\kappa}\hat{a}_{\rm in},\\ \frac{\mathrm{d}\hat{\sigma}_-}{\mathrm{d}t} &= -\left[\mathrm{i}(\omega_{X^-}-\omega)+\frac{\gamma}{2}\right]\hat{\sigma}_- - g\hat{\sigma}_z\hat{a},\end{aligned} \tag{1}$$

where $\omega_{\rm c}$, ω_{X^-}, and ω represent the frequencies of the cavity mode, the X^- dipole operator, and the incident photon, respectively. κ, $\kappa_{\rm s}$, and γ represent the decay rates of the cavity mode, the side leakage, and the negative exciton X^-, respectively. Under a weak excitation condition $\langle\hat{\sigma}_z\rangle \simeq -1$,[73] where the QD spin dominantly occupies the ground state, by combining Eq. (1) with the input-output relation $\hat{a}_{\rm out} = \hat{a}_{\rm in}+\sqrt{\kappa}\hat{a}$, the reflection coefficient for the QD-cavity system can be obtained as

$$r_{\rm h}(\omega) = 1 - \frac{\kappa[\mathrm{i}(\omega_{X^-}-\omega)+\frac{\gamma}{2}]}{[\mathrm{i}(\omega_{X^-}-\omega)+\frac{\gamma}{2}][\mathrm{i}(\omega_{\rm c}-\omega)+\frac{\kappa}{2}+\frac{\kappa_{\rm s}}{2}]+g^2}. \tag{2}$$

When the QD is uncoupled with the cavity, that is, a cold cavity ($g=0$), the reflection coefficient becomes

$$r_0(\omega) = \frac{\mathrm{i}(\omega_{\rm c}-\omega)-\frac{\kappa}{2}+\frac{\kappa_{\rm s}}{2}}{\mathrm{i}(\omega_{\rm c}-\omega)+\frac{\kappa}{2}+\frac{\kappa_{\rm s}}{2}}. \tag{3}$$

The input–output optical process for the interaction between the single-sided QD-cavity system and circularly polarized photons is presented below:

$$\begin{aligned}&|L,\uparrow\rangle \to r_{\rm h}|L,\uparrow\rangle, \quad |L,\downarrow\rangle \to r_0|L,\downarrow\rangle,\\ &|R,\uparrow\rangle \to r_0|R,\uparrow\rangle, \quad |R,\downarrow\rangle \to r_{\rm h}|R,\downarrow\rangle.\end{aligned} \tag{4}$$

3. A parity-check gate

The hyperentangled Bell states of two-photon six-qubit system AA′ in three degrees of freedom (DoFs) can be written as

$$|\varphi\rangle_{\rm AA'} = |\varphi\rangle^{\rm S}_{\rm AA'}\otimes|\varphi\rangle^{\rm P}_{\rm AA'}\otimes|\varphi\rangle^{\rm T}_{\rm AA'}. \tag{5}$$

Here, $|\varphi\rangle^{\rm S}_{\rm AA'}$ is one of the following four Bell states in the spatial-mode DoF:

$$|\phi^{\pm}\rangle^{\rm S}_{\rm AA'} = \frac{1}{\sqrt{2}}(|a_1a_1'\rangle \pm |a_2a_2'\rangle),$$
$$|\psi^{\pm}\rangle^{\rm S}_{\rm AA'} = \frac{1}{\sqrt{2}}(|a_1a_2'\rangle \pm |a_2a_1'\rangle). \quad (6)$$

$|\varphi\rangle^{\rm P}_{\rm AA'}$ is one of the following four Bell states in the polarization DoF:

$$|\phi^{\pm}\rangle^{\rm P}_{\rm AA'} = \frac{1}{\sqrt{2}}(|RR\rangle \pm |LL\rangle),$$
$$|\psi^{\pm}\rangle^{\rm P}_{\rm AA'} = \frac{1}{\sqrt{2}}(|RL\rangle \pm |LR\rangle). \quad (7)$$

$|\varphi\rangle^{\rm T}_{\rm AA'}$ is one of the following four Bell states in the time-bin-mode DoF:

$$|\phi^{\pm}\rangle^{\rm T}_{\rm AA'} = \frac{1}{\sqrt{2}}(|ll\rangle \pm |ss\rangle), \quad |\psi^{\pm}\rangle^{\rm T}_{\rm AA'} = \frac{1}{\sqrt{2}}(|ls\rangle \pm |sl\rangle). \quad (8)$$

Here, the subscripts A and A′ represent two photons A and A′, respectively. S, P, and T represent the spatial, polarization, and time-bin mode DoFs, respectively. $|a_1\rangle$ ($|a_1'\rangle$) and $|a_2\rangle$ ($|a_2'\rangle$) are two spatial modes of the photon A (A′). $|R\rangle$ and $|L\rangle$ stand for the right-circularly and the left-circularly polarized photons, respectively. $|l\rangle$ and $|s\rangle$ stand for the long time-bin and the short time-bin modes, respectively. For simplicity, in the following presentations, the above states can be rewritten as $|\phi^{\pm}\rangle^{X}_{\rm AA'} \equiv |\phi\rangle^{X}_{\rm AA'}$, $|\psi^{\pm}\rangle^{X}_{\rm AA'} \equiv |\psi\rangle^{X}_{\rm AA'}$, $(X = {\rm S, P, T})$. Suppose that the electron spins of three QD-cavity systems are initially prepared in the states $|+\rangle_1 = |+\rangle_2 = |+\rangle_3 = \frac{1}{\sqrt{2}}(|\uparrow\rangle + |\downarrow\rangle)$. The principle of our proposal is given in detail as follows.

Firstly, as shown in the left part of Fig. 2, the photon pair AA′ is injected into the quantum circuit of the spatial parity-check gate (S-PCG). The photon A (A′) in spatial mode $|a_1\rangle$ ($|a_1'\rangle$) passes directly through a wave-form corrector (WFC), which maps $|R\rangle \to \frac{p}{2}(r_{\rm h} - r_0)|R\rangle$ and $|L\rangle \to \frac{p}{2}(r_{\rm h} - r_0)|L\rangle$. Next, the photon A (A′) in spatial mode $|a_2\rangle$ ($|a_2'\rangle$) passes through a circularly polarized beam splitter (CPBS), which transmits the $|R\rangle$-polarized and reflects the $|L\rangle$-polarized components of the two photons AA′. The component $|R\rangle$ ($|L\rangle$) experiences the operations in the sequence ${\rm HWP}^{67.5^\circ} \to {\rm QD}_1$-cavity system $\to {\rm HWP}^{22.5^\circ}$ (${\rm HWP}^{67.5^\circ} \to {\rm QD}_1$-cavity system $\to {\rm HWP}^{112.5^\circ}$), and the two components $|L\rangle$ and $|R\rangle$ will converge on another CPBS again. The S-PCG is finished. The ${\rm HWP}^{22.5^\circ}$, ${\rm HWP}^{67.5^\circ}$, and ${\rm HWP}^{112.5^\circ}$ represent half-wave plates oriented at $\theta = 22.5^\circ$, $\theta = 67.5^\circ$, and $\theta = 112.5^\circ$, respectively, and they complete the operations

$$|R\rangle \longrightarrow \cos 2\theta|R\rangle + \sin 2\theta|L\rangle,$$
$$|L\rangle \longrightarrow \sin 2\theta|R\rangle - \cos 2\theta|L\rangle. \quad (9)$$

Therefore, the polarized state $|L\rangle$ ($|R\rangle$) of the photon and the electron-spin state of the QD before the click of the D_1 can be

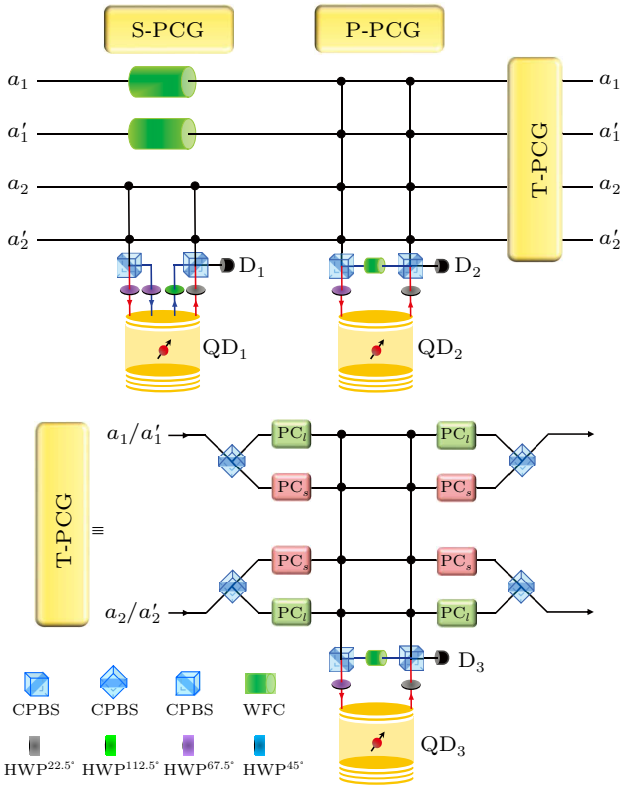


Fig. 2. Schematic diagram of a parity-check gate on two-photons in spatial-polarization-time-bin DoFs. CPBS represents a circularly polarized beam splitter, which transmits the $|R\rangle$-polarized and reflects the $|L\rangle$-polarized components of the photon. The red and blue lines represent the paths of the R-polarized and L-polarized components of the photon, respectively. WFC represents a wave-form corrector, which maps $|R\rangle \to \frac{p}{2}(r_{\rm h} - r_0)|R\rangle$ and $|L\rangle \to \frac{p}{2}(r_{\rm h} - r_0)|L\rangle$. $\rm PC_{\it l}$ ($\rm PC_{\it s}$) is a Pockels cell, which completes a bit-flip operation $|R\rangle \leftrightarrow |L\rangle$ when the l (s) component presents. D is a single-photon detector.

denoted by

$$|R\rangle|\pm\rangle \longrightarrow x|R\rangle|\mp\rangle + y|L\rangle|\pm\rangle,$$
$$|L\rangle|\pm\rangle \longrightarrow x|L\rangle|\mp\rangle + y|R\rangle|\pm\rangle. \quad (10)$$

Here, $|\pm\rangle \equiv \frac{1}{\sqrt{2}}(|\uparrow\rangle \pm |\downarrow\rangle)$, $x = \frac{p}{2}(r_{\rm h} - r_0)$, $y = \frac{p}{2}(r_0 + r_{\rm h}) + \sqrt{1-p^2}$, and p^2 is the rate of the interaction between the $\rm QD_1$-cavity system and the incident photon. Obviously, the left (right)-circularly polarized photon $|L\rangle$ ($|R\rangle$) possesses two output modes no matter what the electron-spin state is. If the output photon $|L\rangle$ ($|R\rangle$) is transformed into the right (left)-circularly polarized photon $|R\rangle$ ($|L\rangle$), it will trigger the $\rm D_1$ and the electron-spin state of the $\rm QD_1$ will remain unchanged to be recycled in the next round; if the output photon $|L\rangle$ ($|R\rangle$) will remain unchanged, the electron-spin state of the QD is accompanied by a phase-flip operation $|+\rangle \leftrightarrow |-\rangle$. Based on Eq. (10), when the $\rm D_1$ in the quantum circuits of the S-PCG responds, it means that the errors originating from the imperfect photon-spin interaction are filtered by the second CPBS and heralded by the $\rm D_1$. When the $\rm D_1$ is not clicked, the states of the hybrid system consisting of two photons A (A′) and the electron spins of three QDs can be written as evolved into

$$|\phi\rangle^{\rm S}_{\rm AA'}\otimes|\varphi\rangle^{\rm P}_{\rm AA'}|\varphi\rangle^{\rm T}_{\rm AA'}|+\rangle_1|+\rangle_2|+\rangle_3 \xrightarrow{\text{S-PCG}} x^2|\phi\rangle^{\rm S}_{\rm AA'}\otimes|\varphi\rangle^{\rm P}_{\rm AA'}|\varphi\rangle^{\rm T}_{\rm AA'}|+\rangle_1|+\rangle_2|+\rangle_3,$$
$$|\psi\rangle^{\rm S}_{\rm AA'}\otimes|\varphi\rangle^{\rm P}_{\rm AA'}|\varphi\rangle^{\rm T}_{\rm AA'}|+\rangle_1|+\rangle_2|+\rangle_3 \xrightarrow{\text{S-PCG}} x^2|\psi\rangle^{\rm S}_{\rm AA'}\otimes|\varphi\rangle^{\rm P}_{\rm AA'}|\varphi\rangle^{\rm T}_{\rm AA'}|-\rangle_1|+\rangle_2|+\rangle_3. \quad (11)$$

Based on Eq. (11), we distinguish even-parity state $|\phi\rangle^{\rm S}_{\rm AA'}$ from odd-parity state $|\psi\rangle^{\rm S}_{\rm AA'}$ by the electron-spin state of $\rm QD_1$, which correspond to $|+\rangle$ and $|-\rangle$, respectively.

Secondly, as shown in the middle of the quantum circuit in Fig. 2, the photon pair $\rm AA'$ is injected into the quantum circuit of the polarization parity-check gate (P-PCG). After two photons $\rm AA'$ pass through the first CPBS, the component $|L\rangle$ passes directly through the WFC, and the component $|R\rangle$ experiences the operations in the sequence $\rm HWP^{67.5^\circ}\rightarrow QD_2$-cavity system $\rightarrow \rm HWP^{22.5^\circ}$. Then the two components $|L\rangle$ and $|R\rangle$ will converge on the second CPBS again. The P-PCG is finished. When the $\rm D_2$ is not clicked, the states of the hybrid system consisting of two photons A ($\rm A'$) and the electron spins of three QDs can be written as

$$|\phi\rangle^{\rm S}_{\rm AA'}|\phi\rangle^{\rm P}_{\rm AA'}\otimes|\varphi\rangle^{\rm T}_{\rm AA'}|+\rangle_1|+\rangle_2|+\rangle_3 \xrightarrow{\text{S-P-PCG}} x^4|\phi\rangle^{\rm S}_{\rm AA'}|\phi\rangle^{\rm P}_{\rm AA'}\otimes|\varphi\rangle^{\rm T}_{\rm AA'}|+\rangle_1|+\rangle_2|+\rangle_3,$$
$$|\phi\rangle^{\rm S}_{\rm AA'}|\psi\rangle^{\rm P}_{\rm AA'}\otimes|\varphi\rangle^{\rm T}_{\rm AA'}|+\rangle_1|+\rangle_2|+\rangle_3 \xrightarrow{\text{S-P-PCG}} x^4|\phi\rangle^{\rm S}_{\rm AA'}|\psi\rangle^{\rm P}_{\rm AA'}\otimes|\varphi\rangle^{\rm T}_{\rm AA'}|+\rangle_1|-\rangle_2|+\rangle_3,$$
$$|\psi\rangle^{\rm S}_{\rm AA'}|\phi\rangle^{\rm P}_{\rm AA'}\otimes|\varphi\rangle^{\rm T}_{\rm AA'}|+\rangle_1|+\rangle_2|+\rangle_3 \xrightarrow{\text{S-P-PCG}} x^4|\psi\rangle^{\rm S}_{\rm AA'}|\phi\rangle^{\rm P}_{\rm AA'}\otimes|\varphi\rangle^{\rm T}_{\rm AA'}|-\rangle_1|+\rangle_2|+\rangle_3,$$
$$|\psi\rangle^{\rm S}_{\rm AA'}|\psi\rangle^{\rm P}_{\rm AA'}\otimes|\varphi\rangle^{\rm T}_{\rm AA'}|+\rangle_1|+\rangle_2|+\rangle_3 \xrightarrow{\text{S-P-PCG}} x^4|\psi\rangle^{\rm S}_{\rm AA'}|\psi\rangle^{\rm P}_{\rm AA'}\otimes|\varphi\rangle^{\rm T}_{\rm AA'}|-\rangle_1|-\rangle_2|+\rangle_3. \quad (12)$$

Based on Eq. (12), we distinguish even-parity state $|\phi\rangle^{\rm P}_{\rm AA'}$ from odd-parity state $|\psi\rangle^{\rm P}_{\rm AA'}$ by the electron-spin state of $\rm QD_2$, which correspond to $|+\rangle$ and $|-\rangle$, respectively.

Thirdly, as shown in the right part of Fig. 2, the photon pair $\rm AA'$ are injected into the quantum circuit of the time-bin parity-check gate (T-PCG), which is composed of the P-PCG and some PCs in essence. After the component $|R\rangle$ and the photon component $|L\rangle$ of the two photons $\rm AA'$ pass through the $\rm PC_{\it s}$ and $\rm PC_{\it l}$, respectively, we find that the time-bin state $|l\rangle$ ($|s\rangle$) is transformed into the polarized states $|R\rangle$ ($|L\rangle$) with the same probability. Therefore, the parity outcome of the time-bin DoF is reflected through that of the polarized DoF of the two-photon system resorting to the P-PCG. $\rm PC_{\it l}$ ($\rm PC_{\it s}$) is a Pockels cell, which completes a bit-flip operation when the l (s) component presents. Then two components $|R\rangle$ and $|L\rangle$ of the two photons $\rm AA'$ will pass through the $\rm PC_{\it s}$ and $\rm PC_{\it l}$ again, respectively. The T-PCG is finished. When the $\rm D_3$ is not clicked, the evolutions of the whole system consisting of two photons A ($\rm A'$) and the electron spins of three QDs are described as follows:

$$|\phi\rangle^{\rm S}_{\rm AA'}|\phi\rangle^{\rm P}_{\rm AA'}|\phi\rangle^{\rm T}_{\rm AA'}|+\rangle_1|+\rangle_2|+\rangle_3 \xrightarrow{\text{S–P–T-PCG}} x^6|\phi\rangle^{\rm S}_{\rm AA'}|\phi\rangle^{\rm P}_{\rm AA'}|\phi\rangle^{\rm T}_{\rm AA'}|+\rangle_1|+\rangle_2|+\rangle_3,$$
$$|\phi\rangle^{\rm S}_{\rm AA'}|\phi\rangle^{\rm P}_{\rm AA'}|\psi\rangle^{\rm T}_{\rm AA'}|+\rangle_1|+\rangle_2|+\rangle_3 \xrightarrow{\text{S–P–T-PCG}} x^6|\phi\rangle^{\rm S}_{\rm AA'}|\phi\rangle^{\rm P}_{\rm AA'}|\psi\rangle^{\rm T}_{\rm AA'}|+\rangle_1|+\rangle_2|-\rangle_3,$$
$$|\phi\rangle^{\rm S}_{\rm AA'}|\psi\rangle^{\rm P}_{\rm AA'}|\phi\rangle^{\rm T}_{\rm AA'}|+\rangle_1|+\rangle_2|+\rangle_3 \xrightarrow{\text{S–P–T-PCG}} x^6|\phi\rangle^{\rm S}_{\rm AA'}|\psi\rangle^{\rm P}_{\rm AA'}|\phi\rangle^{\rm T}_{\rm AA'}|+\rangle_1|-\rangle_2|+\rangle_3,$$
$$|\phi\rangle^{\rm S}_{\rm AA'}|\psi\rangle^{\rm P}_{\rm AA'}|\psi\rangle^{\rm T}_{\rm AA'}|+\rangle_1|+\rangle_2|+\rangle_3 \xrightarrow{\text{S–P–T-PCG}} x^6|\phi\rangle^{\rm S}_{\rm AA'}|\psi\rangle^{\rm P}_{\rm AA'}|\psi\rangle^{\rm T}_{\rm AA'}|+\rangle_1|-\rangle_2|-\rangle_3,$$
$$|\psi\rangle^{\rm S}_{\rm AA'}|\phi\rangle^{\rm P}_{\rm AA'}|\phi\rangle^{\rm T}_{\rm AA'}|+\rangle_1|+\rangle_2|+\rangle_3 \xrightarrow{\text{S–P–T-PCG}} x^6|\psi\rangle^{\rm S}_{\rm AA'}|\phi\rangle^{\rm P}_{\rm AA'}|\phi\rangle^{\rm T}_{\rm AA'}|-\rangle_1|+\rangle_2|+\rangle_3,$$
$$|\psi\rangle^{\rm S}_{\rm AA'}|\phi\rangle^{\rm P}_{\rm AA'}|\psi\rangle^{\rm T}_{\rm AA'}|+\rangle_1|+\rangle_2|+\rangle_3 \xrightarrow{\text{S–P–T-PCG}} x^6|\psi\rangle^{\rm S}_{\rm AA'}|\phi\rangle^{\rm P}_{\rm AA'}|\psi\rangle^{\rm T}_{\rm AA'}|-\rangle_1|+\rangle_2|-\rangle_3,$$
$$|\psi\rangle^{\rm S}_{\rm AA'}|\psi\rangle^{\rm P}_{\rm AA'}|\phi\rangle^{\rm T}_{\rm AA'}|+\rangle_1|+\rangle_2|+\rangle_3 \xrightarrow{\text{S–P–T-PCG}} x^6|\psi\rangle^{\rm S}_{\rm AA'}|\psi\rangle^{\rm P}_{\rm AA'}|\phi\rangle^{\rm T}_{\rm AA'}|-\rangle_1|-\rangle_2|+\rangle_3,$$
$$|\psi\rangle^{\rm S}_{\rm AA'}|\psi\rangle^{\rm P}_{\rm AA'}|\psi\rangle^{\rm T}_{\rm AA'}|+\rangle_1|+\rangle_2|+\rangle_3 \xrightarrow{\text{S–P–T-PCG}} x^6|\psi\rangle^{\rm S}_{\rm AA'}|\psi\rangle^{\rm P}_{\rm AA'}|\psi\rangle^{\rm T}_{\rm AA'}|-\rangle_1|-\rangle_2|-\rangle_3. \quad (13)$$

Based on Eq. (13), we distinguish the even-parity state $|\phi\rangle^{\rm T}_{\rm AA'}$ from the odd-parity state $|\psi\rangle^{\rm T}_{\rm AA'}$ by the electron-spin state of $\rm QD_3$, which correspond to $|+\rangle$ and $|-\rangle$, respectively. As for the time-bin DoF, the time-bin states $|l\rangle$ ($|s\rangle$)) are transformed into the polarized states $|R\rangle$ ($|L\rangle$) with the same probability by the quantum circuit composed of CPBS and $\rm PC_{\it l}$ ($\rm PC_{\it s}$), so that the parity state of the time-bin DoF can be obtained by resorting to the P-PCG.

Finally, we measure the states of three-electron spins in the orthogonal basis $\{|+\rangle_k,|-\rangle_k\}$ $(k=1,2,3)$. If the elec-

tron spin is in the state $|+\rangle_k$, $(k=1,2,3)$, the two photons AA' are projected into the spatial-mode (polarization or time-bin) even-parity state $|\phi\rangle^{S}_{AA'}$ ($|\phi\rangle^{P}_{AA'}$ or $|\phi\rangle^{T}_{AA'}$); if the electron spin is in the state $|-\rangle_k$, $(k=1,2,3)$, the photons AA' are projected into the spatial-mode (polarization or time-bin) odd-parity state $|\psi\rangle^{S}_{AA'}$ ($|\psi\rangle^{P}_{AA'}$ or $|\psi\rangle^{T}_{AA'}$). That is, the S–P–T-PCG for the two-photon system is three individual procedures, S-PCG, P-PCG, and T-PCG. When the D_k $(k=1,2,3)$ in the quantum circuits of the S–P–T-PCG responds, it means that the errors originating from the imperfect photon-spin interaction are filtered by the second CPBS and heralded by the D_k $(k=1,2,3)$. Therefore, the fidelity of the S–P–T-PCG gate is near unity in principle owing to the practical reflection coefficient being a global coefficient, which means the efficiency of the S–P–T-PCG gate is $\eta=|x|^{12}$.

4. Swap gate

4.1. P–P-swap gate between the polarization states of two photons

The polarization–polarization swap (P–P-swap) gate aims to swap the polarized states of two photons without affecting the spatial-mode and time-bin states. Suppose that the electron spin of a QD is initially prepared in the state $|+\rangle$ and two photons AB are prepared in an arbitrary state

$$|\varphi_{ABe}\rangle=|\varphi\rangle^{P}_{A}\otimes|\varphi\rangle^{P}_{B}\otimes|\varphi\rangle^{Y}_{A}\otimes|\varphi\rangle^{Y}_{B}\otimes|+\rangle. \tag{14}$$

Here,

$$\begin{aligned}
|\varphi\rangle^{P}_{A} &= \alpha_1|R\rangle+\alpha_2|L\rangle,\ \ |\varphi\rangle^{P}_{B}=\beta_1|R\rangle+\beta_2|L\rangle,\\
|\varphi\rangle^{Y}_{A} &= (\gamma_1|a_1\rangle+\gamma_2|a_2\rangle)\otimes(\delta_1|l\rangle+\delta_2|s\rangle),\\
|\varphi\rangle^{Y}_{B} &= (\varepsilon_1|b_1\rangle+\varepsilon_2|b_2\rangle)\otimes(\varepsilon_1|l\rangle+\varepsilon_2|s\rangle).
\end{aligned} \tag{15}$$

The complex coefficients conform to the normalization principle, i.e., $|P_1|^2+|P_2|^2=1$ $(P=\alpha,\beta,\gamma,\delta,\varepsilon,\varepsilon)$.

First, the photon pair AB is injected into the quantum circuit as shown in Fig. 3(a). After two photons AB pass through the $CPBS_1$, the component $|R\rangle$ passes directly through the WFC_1, and the component $|L\rangle$ experiences the operations in the sequence $HWP^{67.5^\circ}\rightarrow$ QD-cavity system $\rightarrow HWP^{112.5^\circ}$ (blue line). Then the two components $|L\rangle$ and $|R\rangle$ will converge on the $CPBS_2$ again. When the D_1' is not clicked, the state of the whole system is transformed from $|\varphi_{ABe}\rangle$ to

$$\begin{aligned}
|\varphi\rangle_1 &= x^2\big(\alpha_1\beta_1|RR\rangle_{AB}|+\rangle+\alpha_1\beta_1|RL\rangle_{AB}|-\rangle\\
&\quad+\alpha_1\beta_1|LR\rangle_{AB}|-\rangle+\alpha_1\beta_1|LL\rangle_{AB}|+\rangle\big)\\
&\quad\otimes|\varphi\rangle^{Y}_{A}\otimes|\varphi\rangle^{Y}_{B}.
\end{aligned} \tag{16}$$

Then, after the photon pair AB passes through the half-wave plate $HWP^{22.5^\circ}$, a Hadamard operation H^e, which completes the transformations $|\uparrow\rangle\rightarrow(|\uparrow\rangle+|\downarrow\rangle)/\sqrt{2}$ and $|\uparrow\rangle\rightarrow(|\uparrow\rangle-|\downarrow\rangle)/\sqrt{2}$, is performed on the electron spin of the QD by using a $\pi/2$ microwave pulse.[68,69] Then the two photons AB repeat the above operation again (red line). That is, the two photons AB pass through the $CPBS_3$, the component $|R\rangle$ passes directly through the WFC_2 and the component $|L\rangle$ experiences the operations in the sequence $HWP^{67.5^\circ}\rightarrow$ QD-cavity system $\rightarrow HWP^{112.5^\circ}$. Then the two components $|L\rangle$ and $|R\rangle$ will converge on the $CPBS_4$. After the two photons AB pass through the half-wave plate $HWP^{22.5^\circ}$ again, a Hadamard operation H^e is applied on the electron spin of the QD again. When the D_2' is not clicked, the state of the whole system becomes

$$\begin{aligned}
|\varphi\rangle_2 &= x^4\big[(\beta_1|R\rangle+\beta_2|L\rangle)_A(\alpha_1|R\rangle+\alpha_2|L\rangle)_B|\uparrow\rangle\\
&\quad+(\beta_1|R\rangle-\beta_2|L\rangle)_A(\alpha_1|R\rangle-\alpha_2|L\rangle)_B|\downarrow\rangle\big]\\
&\quad\otimes|\varphi\rangle^{Y}_{A}\otimes|\varphi\rangle^{Y}_{B}.
\end{aligned} \tag{17}$$

Finally, we measure the electron-spin state of the QD-cavity system with the basis $\{|\uparrow\rangle,|\downarrow\rangle\}$. If the measurement result of the electron-spin state is $|\uparrow\rangle$, the state of the two photons is transformed into

$$\begin{aligned}
|\varphi_{AB}\rangle &= x^4(\beta_1|R\rangle+\beta_2|L\rangle)_A(\alpha_1|R\rangle+\alpha_2|L\rangle)_B\\
&\quad\otimes|\varphi\rangle^{Y}_{A}\otimes|\varphi\rangle^{Y}_{B}.
\end{aligned} \tag{18}$$

If the measurement result is $|\downarrow\rangle$, phase-flip operations $\sigma_z^P=|R\rangle\langle R|-|L\rangle\langle L|$ are performed on the polarized DoF of the two photons A and B to obtain the above same state shown in Eq. (18). Obviously, the polarized states of the photons A and B exchange perfectly with single-qubit feedback based on the outcomes of the electron spin. In our P–P-swap gate, the click of the single-photon detector heralds the failure of the gate. Once the P–P-swap gate succeeds, its fidelity approaches unity, owing to the practical reflection coefficient being a global coefficient in the final state. The efficiency of the P–P-swap gate is $\eta_P=|x|^8$.

4.2. P–S-swap gate between the spatial and polarized states of one photon

The polarization–spatial swap (P–S-swap) gate aims to swap the polarized and spatial states of one photon without affecting its time-bin state. Suppose that the initial state of the photon A is $|\varphi\rangle^{P}_{A}\otimes|\varphi\rangle^{Y}_{A}$ shown in Eqs. (14) and (15). We inject photon A into the quantum circuit as shown in Fig. 3(b). After photon A passes through the quantum circuit composed of $CPBS_5$, HWP^{45°, and $CPBS_6$ in turn, the state of photon A is transformed into

$$|\varphi_A\rangle_1=(\gamma_1|R\rangle+\gamma_2|L\rangle)(\alpha_1|a_1\rangle+\alpha_2|a_2\rangle)\otimes|\varphi\rangle^{T}_{A}. \tag{19}$$

Obviously, the polarized and spatial states of photon A exchange perfectly with linear optics only.

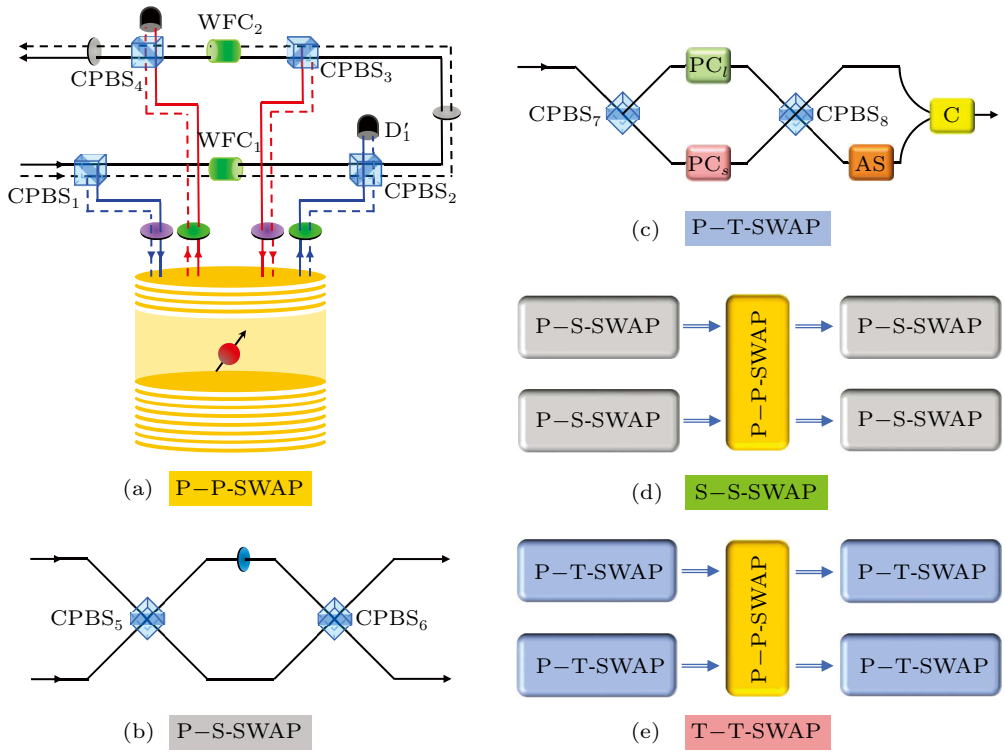


Fig. 3. (a) Schematic diagram of the P–P-swap gate between the polarization states of photon A and photon B. (b) Schematic diagram of the P–S-swap gate between the polarization and the spatial DoFs of one photon. (c) Schematic diagram of the P–T-swap gate between the polarization and the time-bin mode DoFs of one photon. (d) Schematic diagram of the S–S-swap gate between the spatial states of photon A and photon B. (e) Schematic diagram of the T–T-swap gate between the time-bin mode states of photon A and photon B. The solid lines represent the path of photon A and the dotted lines represent the path of photon B. Active switch (AS) completes the flip of the time-bin mode state $|l\rangle \leftrightarrow |s\rangle$. C is the path coupler to combine the two modes, which acts as a quantum eraser to erase the path information without destroying the polarization information. The HWP$^{45^\circ}$ completes the bit-flip operation $|R\rangle \leftrightarrow |L\rangle$.

4.3. P–T-swap gate between the polarized and time-bin states of one photon

The polarization-time-bin swap (P–T-swap) gate is used to swap the polarized and the time-bin states of one photon without affecting the spatial state. The photon A is injected into the quantum circuit as shown in Fig. 3(c). First, after photon A passes through the CPBS$_7$, the component $|R\rangle$ passes through the PC$_s$, and the component $|L\rangle$ passes through the PC$_l$. Then the two components $|L\rangle$ and $|R\rangle$ will converge on the CPBS$_8$. Finally, the photon A in the low path passes through active switches (AS),[74] which complete the flip of the time-bin state, i.e., $|l\rangle \leftrightarrow |s\rangle$, and converge on the upper path by the path coupler C,[75] and the system state of photon A becomes

$$|\varphi_{\rm A}\rangle_2 = (\delta_1|R\rangle + \delta_2|L\rangle)_{\rm A}(\alpha_1|l\rangle + \alpha_2|s\rangle)_{\rm B} \otimes |\varphi\rangle^{\rm S}_{\rm A}. \quad (20)$$

Obviously, the polarized and time-bin states of photon A can be exchanged perfectly with linear optics and AS.

4.4. S–S-swap gate between the spatial states of two photons

The spatial-spatial swap (S–S-swap) gate aims to swap the spatial states of two photons without affecting the polarized and time-bin states. Suppose that the initial states of the photons AB and the electron spin are the same as the P–P-swap gate shown in Eqs. (14) and (15). The S–S-swap gate can be realized by using the P–P-swap gate and some S–P-swap gates shown in Fig. 3(d). In detail, Alice first swaps the polarized states and the spatial states of photon A with the S–P-swap gate and performs the same operation on photon B. Second, Alice swaps the polarized states between photons A and B with the P–P-swap gate. Finally, Alice swaps the polarized states and the spatial states of photons A and B with the P–S-swap gates again. After these operations, the state of the photon pairs becomes

$$\begin{aligned}|\varphi_{\rm AB}\rangle = {} & x^4(\varepsilon_1|a_1\rangle + \varepsilon_2|a_2\rangle)(\gamma_1|b_1\rangle + \gamma_2|b_2\rangle) \\ & \otimes|\varphi\rangle^{\rm P}_{\rm A} \otimes |\varphi\rangle^{\rm P}_{\rm B} \otimes |\varphi\rangle^{\rm T}_{\rm A} \otimes |\varphi\rangle^{\rm T}_{\rm B}. \end{aligned} \quad (21)$$

The fidelity of our S–S-swap gate approaches unity, the same as the P–P-swap gate, and the efficiency of the S–S-swap gate is also $\eta_{\rm S} = |x|^8$.

4.5. T–T-swap gate between the time-bin states of two photons

The time-bin-time-bin swap (T–T-swap) gate aims to swap the time-bin states of two photons without affecting the spatial-mode and polarized states. The T–T-swap gate can be realized by using the P–P-swap gate and some P–T-swap gates

shown in Fig. 3(e), which is similar to the initialization of the S–S-swap gate, only replacing the S–P-swap gate with the P–T-swap gate. After these operations, the state of the photon pairs becomes

$$\begin{aligned}|\varphi_{\rm AB}\rangle &= x^4(\varepsilon_1|l\rangle+\varepsilon_2|s\rangle)_{\rm A}(\delta_1|l\rangle+\delta_2|s\rangle)_{\rm B}\\ &\otimes|\varphi\rangle^{\rm S}_{\rm A}\otimes|\varphi\rangle^{\rm S}_{\rm B}\otimes|\varphi\rangle^{\rm P}_{\rm A}\otimes|\varphi\rangle^{\rm P}_{\rm B}.\end{aligned}\tag{22}$$

Similarly, the fidelity of our T–T-swap gate approaches unity, the same as the P–P-swap (or S–S-swap) gate, and the efficiency of the S–S-swap gate is also $\eta_{\rm T}=|x|^8$.

5. The hyper-EPP for two-photon six-qubit hyperentangled Bell states

In this section, we show our hyper-EPP for mixed hyperentangled Bell states of two-photon systems. Practical transmission of photons in hyperentangled Bell states for high-capacity quantum communication suffers from noise, and both the bit-flip and phase-flip errors will occur randomly. Usually, the phase-flip error can be transformed into the bit-flip error using a bilateral local operation. Therefore, we only discuss the purification for bit-flip errors of two-photon hyperentangled mixed states below. After the transmission of qubits over noisy channels, two two-photon systems AB and A′B′ in mixed hyperentangled Bell states in the spatial, polarization, and time-bin DoFs with bit-flip errors are described as

$$\begin{aligned}\rho_{\rm AB} &= [F_{\rm S}|\phi\rangle^{\rm S}_{\rm AB}\langle\phi|+(1-F_{\rm S})|\psi\rangle^{\rm S}_{\rm AB}\langle\psi|]\\ &\otimes[F_{\rm P}|\phi\rangle^{\rm P}_{\rm AB}\langle\phi|+(1-F_{\rm P})|\psi\rangle^{\rm P}_{\rm AB}\langle\psi|]\\ &\otimes[F_{\rm T}|\phi\rangle^{\rm T}_{\rm AB}\langle\phi|+(1-F_{\rm T})|\psi\rangle^{\rm T}_{\rm AB}\langle\psi|],\\ \rho_{\rm A'B'} &= [F_{\rm S}|\phi\rangle^{\rm S}_{\rm A'B'}\langle\phi|+(1-F_{\rm S})|\psi\rangle^{\rm S}_{\rm A'B'}\langle\psi|]\\ &\otimes[F_{\rm P}|\phi\rangle^{\rm P}_{\rm A'B'}\langle\phi|+(1-F_{\rm P})|\psi\rangle^{\rm P}_{\rm A'B'}\langle\psi|]\\ &\otimes[F_{\rm T}|\phi\rangle^{\rm T}_{\rm A'B'}\langle\phi|+(1-F_{\rm T})|\psi\rangle^{\rm T}_{\rm A'B'}\langle\psi|].\end{aligned}\tag{23}$$

Here, the subscripts AB and A′B′ represent two pairs of photons shared by two remote parties, Alice and Bob. Alice holds photons A and A′, and Bob holds photons B and B′. The initial state of the two identical two-photon six-qubit systems ABA′B′ is expressed as $\rho_0=\rho_{\rm AB}\otimes\rho_{\rm A'B'}$, which can be viewed as a mixture of 64 maximally hyperentangled pure states. Our faithful and efficient hyper-EPP for two-photon hyperentangled systems with the bit-flip errors in three DOFs is divided into two purified steps.

5.1. The first step of our hyper-EPP with S–P–T-PCGs

After Alice performs S–P–T-PCG on the two photons AA′ in three DoFs, and so does Bob on his BB′, the outcomes of the parity are divided into eight cases as shown in Table 1. In case 1, the states of the two pairs of photons AA′ and BB′ are both of the same parity (i.e., even or odd) in three DoFs, which corresponds to the state of identity combinations $|\phi\rangle^{\rm S}_{\rm AB}\otimes|\phi\rangle^{\rm S}_{\rm A'B'}$ or $|\psi\rangle^{\rm S}_{\rm AB}\otimes|\psi\rangle^{\rm S}_{\rm A'B'}$ in the spatial-mode DoF with the probability $F_{\rm S}^2$ or $(1-F_{\rm S})^2$, respectively, the state of identity combinations $|\phi\rangle^{\rm P}_{\rm AB}\otimes|\phi\rangle^{\rm P}_{\rm A'B'}$ or $|\psi\rangle^{\rm P}_{\rm AB}\otimes|\psi\rangle^{\rm P}_{\rm A'B'}$ in the polarized DoF with the probability $F_{\rm P}^2$ or $(1-F_{\rm P})^2$, respectively, and the state of identity combinations $|\phi\rangle^{\rm T}_{\rm AB}\otimes|\phi\rangle^{\rm T}_{\rm A'B'}$ or $|\psi\rangle^{\rm T}_{\rm AB}\otimes|\psi\rangle^{\rm T}_{\rm A'B'}$ in the time-bin DoF with the probability $F_{\rm T}^2$ or $(1-F_{\rm T})^2$, respectively. For simplicity, the above states can be described as $|M\rangle^X_{\rm AB}\otimes|N\rangle^X_{\rm A'B'}$, $M=N\in\{\phi,\psi\}$ and $X\in\{{\rm S},{\rm P},{\rm T}\}$ of case 1. Similarly, the states $|M\rangle^X_{\rm AB}\otimes|N\rangle^X_{\rm A'B'}$, $M\neq N\in\{\phi,\psi\}$ ($X\in\{{\rm S},{\rm P},{\rm T}\}$), $M=N$ ($X\in\{{\rm S},{\rm T}\}$) and $M\neq N$ ($X={\rm P}$), $M=N$ ($X\in\{{\rm S},{\rm P}\}$) and $M\neq N$ ($X={\rm T}$), $M=N$ ($X\in\{{\rm P},{\rm T}\}$) and $M\neq N$ ($X\in\{{\rm S}\}$) ($X={\rm S}$), $M=N$ ($X={\rm S}$) and $M\neq N$ ($X\in\{{\rm P},{\rm T}\}$), $M=N$ ($X={\rm T}$) and $M\neq N$ ($X\in\{{\rm S},{\rm P}\}$), and $M=N$ ($X={\rm P}$) and $M\neq N$ ($X\in\{{\rm S},{\rm T}\}$) correspond to case 2, case 3, case 4, case 5, case 6, case 7, and case 8 in Table 1, respectively, and the outcomes of the parity in three DoFs. In detail, if the two two-photon systems AA′ and BB′ are in even-parity modes in three DoFs in case 1, the state of the four-photon system ABA′B′ is in a new mixed state composed of the six states

$$\begin{aligned}|\Phi\rangle^{\rm S}_1&=\frac{1}{\sqrt{2}}(|a_1b_1a_1'b_1'\rangle+|a_2b_2a_2'b_2'\rangle)_{\rm ABA'B'},\\ |\Phi\rangle^{\rm S}_2&=\frac{1}{\sqrt{2}}(|a_1b_2a_1'b_2'\rangle+||a_2b_1a_2'b_1'\rangle)_{\rm ABA'B'},\\ |\Phi\rangle^{\rm P}_1&=\frac{1}{\sqrt{2}}(|RRRR\rangle+|LLLL\rangle)_{\rm ABA'B'},\\ |\Phi\rangle^{\rm P}_2&=\frac{1}{\sqrt{2}}(|RLRL\rangle+|LRLR\rangle)_{\rm ABA'B'},\\ |\Phi\rangle^{\rm T}_1&=\frac{1}{\sqrt{2}}(|llll\rangle+|ssss\rangle)_{\rm ABA'B'},\\ |\Phi\rangle^{\rm T}_2&=\frac{1}{\sqrt{2}}(|lsls\rangle+|slsl\rangle)_{\rm ABA'B'},\end{aligned}\tag{24}$$

with the probabilities of $\frac{1}{2}F_{\rm S}^2$, $\frac{1}{2}(1-F_{\rm S})^2$, $\frac{1}{2}F_{\rm P}^2$, $\frac{1}{2}(1-F_{\rm P})^2$, $\frac{1}{2}F_{\rm T}^2$, $\frac{1}{2}(1-F_{\rm T})^2$, respectively. If the two two-photon systems AA′ and BB′ are in odd-parity modes in three DoFs in case 1, the state of the four-photon system ABA′B′ is in a new mixed state composed of the six states

$$\begin{aligned}|\Psi\rangle^{\rm S}_1&=\frac{1}{\sqrt{2}}(|a_1b_1a_2'b_2'\rangle+|a_2b_2a_1'b_1'\rangle)_{\rm ABA'B'},\\ |\Psi\rangle^{\rm S}_2&=\frac{1}{\sqrt{2}}(|a_1b_2a_2'b_1'\rangle+|a_2b_1a_1'b_2'\rangle)_{\rm ABA'B'},\\ |\Psi\rangle^{\rm P}_1&=\frac{1}{\sqrt{2}}(|RRLL\rangle+|LLRR\rangle)_{\rm ABA'B'},\\ |\Psi\rangle^{\rm P}_2&=\frac{1}{\sqrt{2}}(|RLLR\rangle+|LRRL\rangle)_{\rm ABA'B'},\\ |\Psi\rangle^{\rm T}_1&=\frac{1}{\sqrt{2}}(|llss\rangle+|ssll\rangle)_{\rm ABA'B'},\\ |\Psi\rangle^{\rm T}_2&=\frac{1}{\sqrt{2}}(|lssl\rangle+|slls\rangle)_{\rm ABA'B'},\end{aligned}\tag{25}$$

with the probabilities of $(1/2)F_{\rm S}^2$, $(1/2)(1-F_{\rm S})^2$, $(1/2)F_{\rm P}^2$, $(1/2)(1-F_{\rm P})^2$, $(1/2)F_{\rm T}^2$, and $(1/2)(1-F_{\rm T})^2$, respectively. The odd-parity states $|\Psi\rangle_1^{\rm S}$ and $|\Psi\rangle_2^{\rm S}$ can be transformed into $|\Phi\rangle_1^{\rm S}$ and $|\Phi\rangle_2^{\rm S}$ with the same probability as the even-parity ones in turn by performing bit-flip operations $\sigma_x^{\rm S} = |b_1\rangle\langle b_1| + |b_2\rangle\langle b_2|$ on the two photons A′B′ in the spatial DoF. As can those in the polarization and the time-bin mode DoFs ($\sigma_x^{\rm P} = |R\rangle\langle L| + |L\rangle\langle R|$ and $\sigma_x^{\rm T} = |l\rangle\langle s| + |s\rangle\langle l|$). In this way, Alice and Bob obtain similar outcomes when they both get either an even parity or an odd parity with S–P–T-PCGs. We only discuss the case where the system is in the even-parity state below.

Table 1. The results of the parity with S–P–T-PCGs on the photons AB and A′B′ in three DoFs and the output states of the two photons AB corresponding to their probabilities.

		AB and A′B′					
Case	DoF	Bell states	Parity mode	State	Probability	State	Probability
1	S	$\|\phi\rangle_{\rm AB}^{\rm S}\otimes\|\phi\rangle_{\rm A'B'}^{\rm S}$ or $\|\psi\rangle_{\rm AB}^{\rm S}\otimes\|\psi\rangle_{\rm A'B'}^{\rm S}$	same	$\|\phi\rangle_{\rm AB}^{\rm S}$	$F_{\rm S}^2$	$\|\psi\rangle_{\rm AB}^{\rm S}$	$(1-F_{\rm S})^2$
	P	$\|\phi\rangle_{\rm AB}^{\rm P}\otimes\|\phi\rangle_{\rm A'B'}^{\rm P}$ or $\|\psi\rangle_{\rm AB}^{\rm P}\otimes\|\psi\rangle_{\rm A'B'}^{\rm P}$	same	$\|\phi\rangle_{\rm AB}^{\rm P}$	$F_{\rm P}^2$	$\|\psi\rangle_{\rm AB}^{\rm P}$	$(1-F_{\rm P})^2$
	T	$\|\phi\rangle_{\rm AB}^{\rm T}\otimes\|\phi\rangle_{\rm A'B'}^{\rm T}$ or $\|\psi\rangle_{\rm AB}^{\rm T}\otimes\|\psi\rangle_{\rm A'B'}^{\rm T}$	same	$\|\phi\rangle_{\rm AB}^{\rm T}$	$F_{\rm T}^2$	$\|\psi\rangle_{\rm AB}^{\rm T}$	$(1-F_{\rm T})^2$
2	S	$\|\phi\rangle_{\rm AB}^{\rm S}\otimes\|\psi\rangle_{\rm A'B'}^{\rm S}$ or $\|\psi\rangle_{\rm AB}^{\rm S}\otimes\|\phi\rangle_{\rm A'B'}^{\rm S}$	different	$\|\phi\rangle_{\rm AB}^{\rm S}$	$F_{\rm S}(1-F_{\rm S})$	$\|\psi\rangle_{\rm AB}^{\rm S}$	$F_{\rm S}(1-F_{\rm S})$
	P	$\|\phi\rangle_{\rm AB}^{\rm P}\otimes\|\psi\rangle_{\rm A'B'}^{\rm P}$ or $\|\psi\rangle_{\rm AB}^{\rm P}\otimes\|\phi\rangle_{\rm A'B'}^{\rm P}$	different	$\|\phi\rangle_{\rm AB}^{\rm P}$	$F_{\rm P}(1-F_{\rm P})$	$\|\psi\rangle_{\rm AB}^{\rm P}$	$F_{\rm P}(1-F_{\rm P})$
	T	$\|\phi\rangle_{\rm AB}^{\rm T}\otimes\|\psi\rangle_{\rm A'B'}^{\rm T}$ or $\|\psi\rangle_{\rm AB}^{\rm T}\otimes\|\phi\rangle_{\rm A'B'}^{\rm T}$	different	$\|\phi\rangle_{\rm AB}^{\rm T}$	$F_{\rm T}(1-F_{\rm T})$	$\|\psi\rangle_{\rm AB}^{\rm T}$	$F_{\rm T}(1-F_{\rm T})$
3	S	$\|\phi\rangle_{\rm AB}^{\rm S}\otimes\|\phi\rangle_{\rm A'B'}^{\rm S}$ or $\|\psi\rangle_{\rm AB}^{\rm S}\otimes\|\psi\rangle_{\rm A'B'}^{\rm S}$	same	$\|\phi\rangle_{\rm AB}^{\rm S}$	$F_{\rm S}^2$	$\|\psi\rangle_{\rm AB}^{\rm S}$	$(1-F_{\rm S})^2$
	P	$\|\phi\rangle_{\rm AB}^{\rm P}\otimes\|\psi\rangle_{\rm A'B'}^{\rm P}$ or $\|\psi\rangle_{\rm AB}^{\rm P}\otimes\|\phi\rangle_{\rm A'B'}^{\rm P}$	different	$\|\phi\rangle_{\rm AB}^{\rm P}$	$F_{\rm P}(1-F_{\rm P})$	$\|\psi\rangle_{\rm AB}^{\rm P}$	$F_{\rm P}(1-F_{\rm P})$
	T	$\|\phi\rangle_{\rm AB}^{\rm T}\otimes\|\phi\rangle_{\rm A'B'}^{\rm T}$ or $\|\psi\rangle_{\rm AB}^{\rm T}\otimes\|\psi\rangle_{\rm A'B'}^{\rm T}$	same	$\|\phi\rangle_{\rm AB}^{\rm T}$	$F_{\rm T}^2$	$\|\psi\rangle_{\rm AB}^{\rm T}$	$(1-F_{\rm T})^2$
4	S	$\|\phi\rangle_{\rm AB}^{\rm S}\otimes\|\phi\rangle_{\rm A'B'}^{\rm S}$ or $\|\psi\rangle_{\rm AB}^{\rm S}\otimes\|\psi\rangle_{\rm A'B'}^{\rm S}$	same	$\|\phi\rangle_{\rm AB}^{\rm S}$	$F_{\rm S}^2$	$\|\psi\rangle_{\rm AB}^{\rm S}$	$(1-F_{\rm S})^2$
	P	$\|\phi\rangle_{\rm AB}^{\rm P}\otimes\|\phi\rangle_{\rm A'B'}^{\rm P}$ or $\|\psi\rangle_{\rm AB}^{\rm P}\otimes\|\psi\rangle_{\rm A'B'}^{\rm P}$	same	$\|\phi\rangle_{\rm AB}^{\rm P}$	$F_{\rm P}^2$	$\|\psi\rangle_{\rm AB}^{\rm P}$	$(1-F_{\rm P})^2$
	T	$\|\phi\rangle_{\rm AB}^{\rm T}\otimes\|\psi\rangle_{\rm A'B'}^{\rm T}$ or $\|\psi\rangle_{\rm AB}^{\rm T}\otimes\|\phi\rangle_{\rm A'B'}^{\rm T}$	different	$\|\phi\rangle_{\rm AB}^{\rm T}$	$F_{\rm T}(1-F_{\rm T})$	$\|\psi\rangle_{\rm AB}^{\rm T}$	$F_{\rm T}(1-F_{\rm T})$
5	S	$\|\phi\rangle_{\rm AB}^{\rm S}\otimes\|\psi\rangle_{\rm A'B'}^{\rm S}$ or $\|\psi\rangle_{\rm AB}^{\rm S}\otimes\|\phi\rangle_{\rm A'B'}^{\rm S}$	different	$\|\phi\rangle_{\rm AB}^{\rm S}$	$F_{\rm S}(1-F_{\rm S})$	$\|\psi\rangle_{\rm AB}^{\rm S}$	$F_{\rm S}(1-F_{\rm S})$
	P	$\|\phi\rangle_{\rm AB}^{\rm P}\otimes\|\phi\rangle_{\rm A'B'}^{\rm P}$ or $\|\psi\rangle_{\rm AB}^{\rm P}\otimes\|\psi\rangle_{\rm A'B'}^{\rm P}$	same	$\|\phi\rangle_{\rm AB}^{\rm P}$	$F_{\rm P}^2$	$\|\psi\rangle_{\rm AB}^{\rm P}$	$(1-F_{\rm P})^2$
	T	$\|\phi\rangle_{\rm AB}^{\rm T}\otimes\|\phi\rangle_{\rm A'B'}^{\rm T}$ or $\|\psi\rangle_{\rm AB}^{\rm T}\otimes\|\psi\rangle_{\rm A'B'}^{\rm T}$	same	$\|\phi\rangle_{\rm AB}^{\rm T}$	$F_{\rm T}^2$	$\|\psi\rangle_{\rm AB}^{\rm T}$	$(1-F_{\rm T})^2$
6	S	$\|\phi\rangle_{\rm AB}^{\rm S}\otimes\|\phi\rangle_{\rm A'B'}^{\rm S}$ or $\|\psi\rangle_{\rm AB}^{\rm S}\otimes\|\psi\rangle_{\rm A'B'}^{\rm S}$	same	$\|\phi\rangle_{\rm AB}^{\rm S}$	$F_{\rm S}^2$	$\|\psi\rangle_{\rm AB}^{\rm S}$	$(1-F_{\rm S})^2$
	P	$\|\phi\rangle_{\rm AB}^{\rm P}\otimes\|\psi\rangle_{\rm A'B'}^{\rm P}$ or $\|\psi\rangle_{\rm AB}^{\rm P}\otimes\|\phi\rangle_{\rm A'B'}^{\rm P}$	different	$\|\phi\rangle_{\rm AB}^{\rm P}$	$F_{\rm P}(1-F_{\rm P})$	$\|\psi\rangle_{\rm AB}^{\rm P}$	$F_{\rm P}(1-F_{\rm P})$
	T	$\|\phi\rangle_{\rm AB}^{\rm T}\otimes\|\psi\rangle_{\rm A'B'}^{\rm T}$ or $\|\psi\rangle_{\rm AB}^{\rm T}\otimes\|\phi\rangle_{\rm A'B'}^{\rm T}$	different	$\|\phi\rangle_{\rm AB}^{\rm T}$	$F_{\rm T}(1-F_{\rm T})$	$\|\psi\rangle_{\rm AB}^{\rm T}$	$F_{\rm T}(1-F_{\rm T})$
7	S	$\|\phi\rangle_{\rm AB}^{\rm S}\otimes\|\psi\rangle_{\rm A'B'}^{\rm S}$ or $\|\psi\rangle_{\rm AB}^{\rm S}\otimes\|\phi\rangle_{\rm A'B'}^{\rm S}$	different	$\|\phi\rangle_{\rm AB}^{\rm S}$	$F_{\rm S}(1-F_{\rm S})$	$\|\psi\rangle_{\rm AB}^{\rm S}$	$F_{\rm S}(1-F_{\rm S})$
	P	$\|\phi\rangle_{\rm AB}^{\rm P}\otimes\|\psi\rangle_{\rm A'B'}^{\rm P}$ or $\|\psi\rangle_{\rm AB}^{\rm P}\otimes\|\phi\rangle_{\rm A'B'}^{\rm P}$	different	$\|\phi\rangle_{\rm AB}^{\rm P}$	$F_{\rm P}(1-F_{\rm P})$	$\|\psi\rangle_{\rm AB}^{\rm P}$	$F_{\rm P}(1-F_{\rm P})$
	T	$\|\phi\rangle_{\rm AB}^{\rm T}\otimes\|\phi\rangle_{\rm A'B'}^{\rm T}$ or $\|\psi\rangle_{\rm AB}^{\rm T}\otimes\|\psi\rangle_{\rm A'B'}^{\rm T}$	same	$\|\phi\rangle_{\rm AB}^{\rm T}$	$F_{\rm T}^2$	$\|\psi\rangle_{\rm AB}^{\rm T}$	$(1-F_{\rm T})^2$
8	S	$\|\phi\rangle_{\rm AB}^{\rm S}\otimes\|\psi\rangle_{\rm A'B'}^{\rm S}$ or $\|\psi\rangle_{\rm AB}^{\rm S}\otimes\|\phi\rangle_{\rm A'B'}^{\rm S}$	different	$\|\phi\rangle_{\rm AB}^{\rm S}$	$F_{\rm S}(1-F_{\rm S})$	$\|\psi\rangle_{\rm AB}^{\rm S}$	$F_{\rm S}(1-F_{\rm S})$
	P	$\|\phi\rangle_{\rm AB}^{\rm P}\otimes\|\phi\rangle_{\rm A'B'}^{\rm P}$ or $\|\psi\rangle_{\rm AB}^{\rm P}\otimes\|\psi\rangle_{\rm A'B'}^{\rm P}$	same	$\|\phi\rangle_{\rm AB}^{\rm P}$	$F_{\rm P}^2$	$\|\psi\rangle_{\rm AB}^{\rm P}$	$(1-F_{\rm P})^2$
	T	$\|\phi\rangle_{\rm AB}^{\rm T}\otimes\|\psi\rangle_{\rm A'B'}^{\rm T}$ or $\|\psi\rangle_{\rm AB}^{\rm T}\otimes\|\phi\rangle_{\rm A'B'}^{\rm T}$	different	$\|\phi\rangle_{\rm AB}^{\rm T}$	$F_{\rm T}(1-F_{\rm T})$	$\|\psi\rangle_{\rm AB}^{\rm T}$	$F_{\rm T}(1-F_{\rm T})$

Subsequently, Alice and Bob detect the photons A′ and B′ in the spatial, polarization, and time-bin mode DoFs with the single-photon measurement devices, shown in Fig. 4, respectively. The states $|\Phi\rangle_1^{\rm S}$, $|\Phi\rangle_2^{\rm S}$, $|\Phi\rangle_1^{\rm P}$, $|\Phi\rangle_2^{\rm P}$, $|\Phi\rangle_1^{\rm T}$, and $|\Phi\rangle_2^{\rm T}$ are changed into the states

$$
\begin{aligned}
|\Phi\rangle_{1'}^{\rm S} &= \frac{1}{2\sqrt{2}}(|a_1b_1\rangle+|a_2b_2\rangle)_{\rm AB}(|a_1'b_1'\rangle+|a_2'b_2'\rangle)_{\rm A'B'}\\
&\quad+(|a_1b_1\rangle-|a_2b_2\rangle)_{\rm AB}(|a_1'b_2'\rangle+|a_2'b_1'\rangle)_{\rm A'B'},\\
|\Phi\rangle_{2'}^{\rm S} &= \frac{1}{2\sqrt{2}}(|a_1b_2\rangle+|a_2b_1\rangle)_{\rm AB}(|a_1'b_1'\rangle-|a_2'b_2'\rangle)_{\rm A'B'}\\
&\quad+(-|a_1b_2\rangle+|a_2b_1\rangle)_{\rm AB}(|a_1'b_2'\rangle-|a_2'b_1'\rangle)_{\rm A'B'},\\
|\Phi\rangle_{1'}^{\rm P} &= \frac{1}{2\sqrt{2}}(|RR\rangle+|LL\rangle)_{\rm AB}(|RR\rangle+|LL\rangle)_{\rm A'B'}\\
&\quad+(|RR\rangle-|LL\rangle)_{\rm AB}(|RL\rangle+|LR\rangle)_{\rm A'B'},\\
|\Phi\rangle_{2'}^{\rm P} &= \frac{1}{2\sqrt{2}}(|RL\rangle+|LR\rangle)_{\rm AB}(|RR\rangle-|LL\rangle)_{\rm A'B'}\\
&\quad+(-|RL\rangle+|LR\rangle)_{\rm AB}(|RL\rangle-|LR\rangle)_{\rm A'B'},\\
|\Phi\rangle_{1'}^{\rm T} &= \frac{1}{2\sqrt{2}}(|ll\rangle+|ss\rangle)_{\rm AB}(|ll\rangle+|ss\rangle)_{\rm A'B'}\\
&\quad+(|ll\rangle-|ss\rangle)_{\rm AB}(|ls\rangle+|sl\rangle)_{\rm A'B'},\\
|\Phi\rangle_{2'}^{\rm T} &= \frac{1}{2\sqrt{2}}(|ls\rangle+|sl\rangle)_{\rm AB}(|ll\rangle-|ss\rangle)_{\rm A'B'}\\
&\quad+(-|ls\rangle+|sl\rangle)_{\rm AB}(|ls\rangle-|sl\rangle)_{\rm A'B'}.
\end{aligned}
\tag{26}
$$

After the two photons A′B′ are detected by single-photon detectors, if the two photons A′B′ are in the even-parity mode in the spatial DoF (in the polarization or time-bin mode DoFs), the first purification step of the hyper-EPP is realized directly. If they are in the odd-parity state in three DoFs, the first step of the hyper-EPP is realized after performing a phase-flip operation $\sigma_z^{\rm S} = |b_1\rangle\langle b_1| - |b_2\rangle\langle b_2|$ on photon B in the spatial DoF, $\sigma_z^{\rm P} = |R\rangle\langle R| - |L\rangle\langle L|$ on photon B in the polarization DoF, and $\sigma_z^{\rm T} = |l\rangle\langle l| - |s\rangle\langle s|$ on photon B in the time-bin DoF, respec-

tively. Thus we obtain the states $|\phi\rangle_{AB}^{S}$ and $|\psi\rangle_{AB}^{S}$ with probability F_S^2 and$(1-F_S)^2$, the states $|\phi\rangle_{AB}^{P}$ and $|\psi\rangle_{AB}^{P}$ with probability F_P^2 and$(1-F_P)^2$, and the states $|\phi\rangle_{AB}^{T}$ and $|\psi\rangle_{AB}^{T}$ with probability F_T^2 and $(1-F_T)^2$, respectively. The same applies to the cases 2–8 shown in Table 1. In case 2, the states of the photons AA′ and BB′ are of different parity in three DoFs. However, Alice and Bob should discard the photon pair AB in this case, as photons AB are now in a mixed state composed of the correct and bit-flip-error states with equal probability $F_X(1-F_X)$ $(X \in \{S,P,T\})$ in each DoF. Cases 3–8 can be used in the second step of our hyper-EPP with swap gates below.

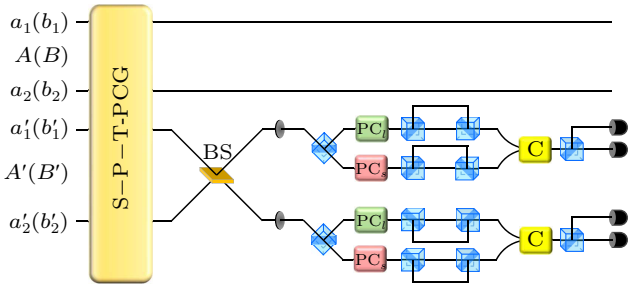


Fig. 4. The first step of our hyper-EPP with S–P–T-PCGs. BS is a 50:50 beam splitter.

5.2. The second step of our hyper-EPP with swap gates

For two-photon systems created in cases 3–8 by the first step of our hyper-EPP, the higher-fidelity hyperentangled photons in three DoFs will be created by the second step of our hyper-EPP with swap gates, which can pump the higher-fidelity states into the same photon pair. This will be used to improve the efficiency of our hyper-EPP. In general, there are six possible purified combinations shown in Table 2.

Suppose that Alice and Bob share the states of two photon pairs AB and A′B′ from cases 3 and 8, respectively, after the first purified step shown in Table 1. Obviously, AB is created from case 3 with higher fidelity in both the spatial and time-bin DoFs, while A′B′ is created from case 8 with higher fidelity in the polarized DoF only. Alice performs a fidelity-unity P–P-swap gate on her photons A and A′, and Bob performs a fidelity-unity P–P swap gate on the photons B and B′ as shown in Fig. 3(a). Using the two P–P swap gates, Alice and Bob complete the purification process of the photon pair AB, by replacing the lower-fidelity polarized state of AB with the higher-fidelity polarized state of A′B′. Now, all the spatial, polarized, and time-bin DoFs of photon pair AB are of higher fidelities, which are the same as those in case 1 in principle. Similarly, if Alice and Bob share the states of two photon pairs AB and A′B′ from cases 8 and 3, respectively, Alice (Bob) performs the fidelity-unity S–S-swap gate and T–T-swap gate on her (his) photons A and A′ (B and B′) in the spatial and time-bin DoFs in turn to get the same outcome as in case 1. The same applies to the other combinations shown in Table 2. In a word, the purpose of the second purified step is to improve the probability of the even-parity Bell state in one or two DoFs by costing some other two-photon systems. Thus, by the swap gates, the fidelities of the two-photon system AB in three DoFs are significantly improved.

Table 2. The six combinations and the corresponding operations of swap gates.

AB	A′B′	S–S-swap	P–P-swap	T–T-swap
case 3	case 8		√	
case 8	case 3	√		√
case 4	case 7			√
case 7	case 4	√	√	
case 5	case 6	√		
case 6	case 5		√	√

5.3. Fidelity and efficiency of our hyper-EPP

After two purified steps, the first round of our hyper-EPP process is completed and the state of the two-photon system AB is changed into

$$\begin{aligned}\rho_{AB} = &\left[f_S|\phi\rangle_{AB}^{S}\langle\phi| + (1-f_S)|\psi\rangle_{AB}^{S}\langle\psi|\right] \\ &\otimes \left[f_P|\phi\rangle_{AB}^{P}\langle\phi| + (1-f_P)|\psi\rangle_{AB}^{P}\langle\psi|\right] \\ &\otimes \left[f_T|\phi\rangle_{AB}^{T}\langle\phi| + (1-f_T)|\psi\rangle_{AB}^{T}\langle\psi|\right], \end{aligned} \tag{27}$$

where $f_S = \frac{F_S^2}{F_S^2+(1-F_S)^2}$, $f_P = \frac{F_P^2}{F_P^2+(1-F_P)^2}$, and $f_T = \frac{F_T^2}{F_T^2+(1-F_T)^2}$. Now, we discuss the fidelity and efficiency of our hyper-EPP. The fidelity of the final state is $F' = f_S \times f_P \times f_T$, which is larger than the initial fidelity $F = F_S \times F_P \times F_T$ as we have assumed $F_S > 0.5$, $F_P > 0.5$, and $F_T > 0.5$. By iterating our hyper-EPP process, the fidelity of the state of the two-photon system can be improved dramatically. The fidelities of the final state are shown in Fig. 5(a) iterating $n = 1, 2, 3$ times for the case with $F_S = F_P = F_T = F$.

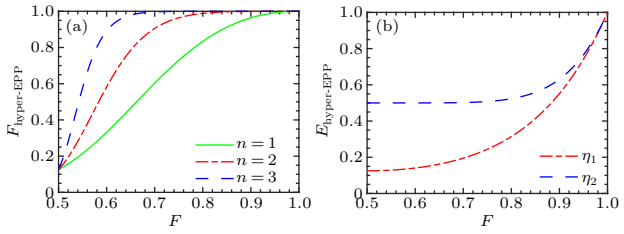


Fig. 5. (a) The fidelity of our hyper-EPP. The green line, red double dash line and blue dotted line represent the reliability of $n = 1, 2, 3$ iterations when $F_S = F_P = F_T = F$, respectively. (b) The efficiency of our hyper-EPP with the same conditions.

The efficiency of an EPP is defined as the probability of obtaining a high-fidelity entangled photon system from a pair of photon systems transmitted over a noisy channel without photon loss. The efficiency of our hyper-EPP after the first step in the first round is

$$\eta_1 = \eta K_S K_P K_T. \tag{28}$$

After the second step, the efficiency of the first round of the hyper-EPP process is

$$\eta_2 = \eta_1 + \eta^2[\eta_P \min\{K_S' K_P K_T, K_S K_P' K_T'\}$$

$$+\eta_{\rm S}\min\{K_{\rm S}K'_{\rm P}K_{\rm T}, K'_{\rm S}K_{\rm P}K'_{\rm T}\}$$
$$+\eta_{\rm T}\min\{K_{\rm S}K_{\rm P}K'_{\rm T}, K'_{\rm S}K'_{\rm P}K_{\rm T}\}], \quad (29)$$

where $K_X = F_X^2 + (1-F_X)^2$, $K'_X = 2F_X(1-F_X)$, (X = S, P, T). Figure 5(b) shows the efficiencies η_1 and η_2 of our hyper-EPP for the cases with $F_{\rm S} = F_{\rm P} = F_{\rm T} = F$ and $\eta = \eta_{\rm S} = \eta_{\rm P} = \eta_{\rm T} = 1$, respectively. It is easily found that the efficiency η_2 in Fig. 5(b) of our hyper-EPP is greatly increased. For the initial fidelities $0.6 < F_{\rm S}, F_{\rm P}, F_{\rm T} < 0.75$, $\eta_2 > 2\eta_1$. Obviously, the initial fidelities in three DoFs are smaller, and the second purified step with quantum swap gates plays an important role in the first round of the hyper-EPP process. Besides, as in all quantum operations, the S–P–T-PCGs, and P–P (S–S or T–T)-swap gates will work with a near-unity fidelity, the hyper-EPP here will be performed faithfully and work without the influence of infidelity.

6. Discussion

The unity-fidelity PCG and the swap gates are two core tools for realizing the faithful hyper-EPP on a two-photon system in the polarization, spatial, and time-bin mode DoFs. The failure of the S–P–T-PCG for photon systems in three DoFs can be heralded by the responses of the single-photon detectors in three QD-cavity systems. Since the errors coming from practical scattering in these quantum circuits are converted into the failure of detection, the fidelity will be unity, in principle, when the S–P–T-PCG succeeds. So will that of our P–P-swap, S–S-swap, and T–T-swap gates.

The efficiency is defined as $\eta = \eta_{\rm out}/\eta_{\rm in}$, where $\eta_{\rm out}$ represents the number of the output photons and $\eta_{\rm in}$ represents the number of the input photons. The efficiency of the PCG for the two-photon system in each DoF whether odd or even parity $\eta_{\rm PCG} = |\frac{p}{2}(r_{\rm h} - r_0)|^4$, shown in Fig. 6(a), is largely constrained by the practical QD-cavity union. The efficiencies of our P–P-swap, S–S-swap, and T–T-swap gates are equal to $\eta_{\rm swap} = \eta_{\rm S} = \eta_{\rm P} = \eta_{\rm T} = |\frac{p}{2}(r_{\rm h} - r_0)|^8$, shown in Fig. 6(b). It can be seen from Figs. 6(a) and 6(b) that the efficiencies are further improved with the increase of parameters $g/\sqrt{\kappa\gamma}$ and p^2. For example, the efficiency of the PCG is improved from $\eta_{\rm PCG} = 93.99\%$ to $\eta_{\rm PCG} = 97.27\%$ as the parameter increases from $g/\sqrt{\kappa\gamma} = 4$ to $g/\sqrt{\kappa\gamma} = 6$ for the fixed parameter $p^2 = 1$, and the efficiency of the swap gate increases from $\eta_{\rm swap} = 88.34\%$ to $\eta_{\rm swap} = 94.61\%$. Similarly, the efficiency could be further increased by increasing the QD-cavity coupling strength and suppressing the cavity side leakage as shown in Figs. 7(a) and 7(b). For example, the efficiency of the PCG is improved from $\eta_{\rm PCG} = 98.90\%$ to $\eta_{\rm PCG} = 99.60\%$ as the parameter increases from $g/\kappa = 3$ to $g/\kappa = 5$ for the fixed parameter $\kappa_{\rm s}/\kappa = 0$, and the efficiency of the swap gate increases from $\eta_{\rm swap} = 97.81\%$ to $\eta_{\rm swap} = 99.2\%$. The efficiencies of the PCG and swap gate are $\eta_{\rm PCG} = 81.93\%$ and $\eta_{\rm swap} = 67.12\%$, respectively, when the parameters for the fixed parameter $\kappa_{\rm s}/\kappa = 0.05$ and $g/\kappa = 5$. Therefore, we can optimize the QD-cavity system by improving the coupling strength of the QD-cavity system and suppressing the cavity side leakage, which can achieve the high efficiency of our scheme.

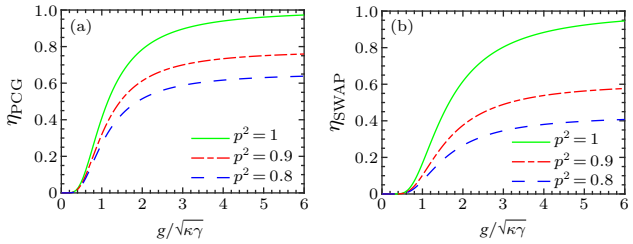


Fig. 6. (a) The efficiency of the PCG and (b) the efficiency of the swap gate with parameters $\kappa_{\rm s} \ll \kappa$ and $\omega = \omega_{\rm c} = \omega_{X^-}$. The green line, red double dash line and blue dotted line represent the efficiency with $p^2 = 1$, 0.9, 0.8, respectively.

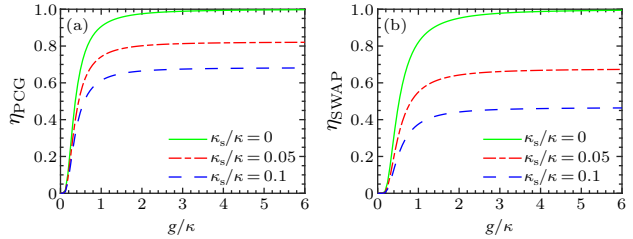


Fig. 7. (a) The efficiency of the PCG and (b) the efficiency of the swap gate with parameters $\gamma = 0.1\kappa$, $\omega = \omega_{\rm c} = \omega_{X^-}$, and $p = 1$. The green line, red double dash line and blue dotted line represent the efficiency with $\kappa_{\rm s}/\kappa = 0$, 0.05, 0.1, respectively.

7. Summary

In summary, we have presented a faithful and efficient hyper-EPP for a two-photon system in the spatial, polarization, and time-bin mode DoFs, resorting to unity-fidelity S–P–T-PCG and the swap gates, which consists of two steps. First, we pick out the effective components (except case 2) from the original mixed state based on S–P–T-PCGs in the first purification step. Interestingly, the useful photon pair obtained from case 1 directly completes the first round of our hyper-EPP. By introducing the swap gate to realize the swapping operation between different photon pairs, two parties in quantum communication can reuse the original photon pairs of cases 3–8 in the first purification step to distill again high-fidelity ones, which significantly improves the efficiency of our hyper-EPP. The fidelities of the S–P–T-PCGs and swap gates used in the two steps are unity, in principle, in practical scattering. The imperfections, such as the finite side leakage of the microcavity and the finite coupling between the QD and the cavity mode, will only reduce the efficiencies in a heralded way, but not affect the fidelities. This makes our hyper-EPP work faithfully for high-capacity long-distance quantum networks. The maximal hyperentanglement state can be achieved by performing multiple rounds of the hyper-EPP in principle. Fur-

thermore, our hyper-EPP could be extended directly to purify multiphoton systems.

Acknowledgments

Project supported by the National Natural Science Foundation of China (Grant No. 61901420 and 11604226), the Shanxi Province Science Foundation for Youths (Grant No. 201901D211235), the Scientific and Technological Innovation Programs of Higher Education Institutions in Shanxi (Grant No. 2019L0507), and the Program of Beijing Municipal Commission of Education of China (Grant Nos. CIT&TCD201904080 and KM201810028005).

References

[1] Ekert A K 1991 *Phys. Rev. Lett.* **67** 661
[2] Zhao Y B, Zhang W L, Wang D, Song X T, Zhou L J and Ding C B 2019 *Chin. Phys. B* **28** 104203
[3] Cui Z X, Zhong W, Zhou L and Sheng Y B 2019 *Sci. Chin. Phys. Mech. Astron.* **62** 110311
[4] Li J J, Wang Y, Li H W and Bao W S 2020 *Chin. Phys. B* **29** 030303
[5] Li X, Yuan H W, Zhang C M and Wang Q 2020 *Chin. Phys. B* **29** 070303
[6] Zhao P, Zhou L, Zhong W and Sheng Y B 2021 *Europhys. Lett.* **135** 40001
[7] Hillery M, Bužek V and Berthiaume A 1999 *Phys. Rev. A* **59** 1829
[8] Luo G F, Zhou R G and Hu W W 2019 *Chin. Phys. B* **28** 040302
[9] Yang L, Liu Y C and Li Y S 2020 *Chin. Phys. B* **29** 060301
[10] Gao Z K, Li T and Li Z H 2020 *Sci. Chin. Phys. Mech. Astron.* **63** 120311
[11] Wang Y, Lou X P, Fan Z, Wang S and Huang G 2022 *Int. J. Theor. Phys.* **61** 24
[12] Chen X X and Huang G 2022 *Int. J. Theor. Phys.* **61** 99
[13] Long G L and Liu X S 2002 *Phys. Rev. A* **65** 032302
[14] Zhang W, Ding D S, Sheng Y B, Zhou L, Shi B S and Guo G C 2017 *Phys. Rev. Lett.* **118** 220501
[15] Zhu F, Zhang W, Sheng Y B and Huang Y D 2017 *Sci. Bull.* **62** 1519
[16] Gao Z K, Li T and Li Z H 2019 *Europhys. Lett.* **125** 40004
[17] Li T and Long G L 2020 *New J. Phys.* **22** 063017
[18] Qi Z T, Li Y H, Huang Y W, Feng J, Zheng Y L and Chen X F 2021 *Light Sci. Appl.* **10** 183
[19] Long G L and Zhang H R 2021 *Sci. Bull.* **66** 1267
[20] Sheng Y B, Zhou L and Long G L 2022 *Sci. Bull.* **67** 367
[21] Liu X, Li Z J, Luo D, Huang C F, Ma D, Geng M M, Wang J W, Zhang Z R and Wei K J 2021 *Sci. Chin. Phys. Mech. Astron.* **64** 120311
[22] Barreiro J T, Langford N K, Peters N A and Kwiat P G. 2005 *Phys. Rev. Lett.* **95** 260501
[23] Ceccarelli R, Vallone G, Martini F D, Mataloni P and Cabello A 2005 *Phys. Rev. Lett.* **103** 160401
[24] Vallone G, Ceccarelli R, Martini F D and Mataloni P 2009 *Phys. Rev. A* **79** 030301
[25] Yabushita A and Kobayashi T 2004 *Phys. Rev. A* **69** 013806
[26] Barreiro J T, Wei T C and Kwiat P G 2008 *Nat. Phys.* **4** 282
[27] Trávníček V, Bartkiewicz K, Černoch A and Lemr K 2008 *Phys. Rev. A* **98** 032307
[28] Simon D S and Sergienko A V 2014 *New J. Phys.* **16** 063052
[29] Chen K L, Che M, Zhang Q, Chen Y A, Goebel A, Chen S, Mair A and Pan J W 2007 *Phys. Rev. Lett.* **99** 120503
[30] Zhou X J, Liu W Q, Wei H R, Zheng Y B and Du F F 2022 *Front. Phys.* **17** 41502
[31] Zhou X J, Liu W Q, Zheng Y B, Wei H R and Du F F 2022 *Ann. Phys.* **534** 2100509
[32] Wang P, Yu C Q, Wang Z X, Yuan R Y, Du F F and Ren B C 2021 *Front. Phys.* **17** 31501
[33] Du F F, Wu Y M, Fan G and Ma Z M 2023 *Ann. Phys.* **535** 2200507
[34] R B C, Wang G Y and Deng F G 2015 *Phys. Rev. A* **91** 032328
[35] Li T and Long G L 2016 *Phys. Rev. A* **94** 022343
[36] Wei H R, Deng F G and Long G L 2016 *Opt. Express* **24** 18619
[37] Du F F and Shi Z R 2019 *Opt. Express* **27** 17493
[38] Han Y H, Cao C, Fan L and Zhang R 2021 *Opt. Express* **29** 20045
[39] Wu Y M, Fan G and Du F F 2022 *Front. Phys.* **17** 51502
[40] Bennett C H, Brassard G, Popescu S, Schumacher B, Smolin J A and Wootters W K 1996 *Phys. Rev. Lett.* **76** 722
[41] Pan J W, Simon C, Brukner Č and Zeilinger A 2001 *Nature* **410** 1067
[42] Zhou L, Liu Z K, Xu Z X, Cui Y L, Ran H J and Sheng Y B 2021 *Quantum Inf. Process.* **20** 257
[43] Sheng Y B, Deng F G and Zhou H Y 2008 *Phys. Rev. A* **77** 042308
[44] Wang C, Zhang Y and Jin G S 2011 *Phys. Rev. A* **84** 032307
[45] Wang C, Zhang Y and Zhang R 2011 *Opt. Express* **19** 25685
[46] Gonta D and van Loock P 2012 *Phys. Rev. A* **86** 052312
[47] Ren B C and Deng F G 2013 *Laser Phys. Lett.* **10** 115201
[48] Wang G Y, Liu Q and Deng F G 2016 *Phys. Rev. A* **94** 032319
[49] Ren B C, Du F F and Deng F G 2014 *Phys. Rev. A* **90** 052309
[50] Wang G Y, Li T, Ai Q, Alsaedi A, Hayat T and Deng F G 2018 *Phys. Rev. Appl.* **10** 054058
[51] Du F F, Liu Y T, Shi Z R, Liang Y X, Tang J and Liu J 2019 *Opt. Express* **27** 27046
[52] Zhou L and Sheng Y B 2016 *Scientific Reports* **6** 28813
[53] Zhou L and Sheng Y B 2017 *Annals of Physics* **385** 10
[54] Zhang H, Liu Q, Xu X S, Xiong J, Alsaedi A, Hayat T and Deng F G 2017 *Phys. Rev. A* **96** 052330
[55] Miguel-Ramiro J and Dür W 2018 *Phys. Rev. A* **98** 042309
[56] Sheng Y B and Deng F G 2010 *Phys. Rev. A* **81** 032307
[57] Sheng Y B and Deng F G 2010 *Phys. Rev. A* **82** 044305
[58] Yan P S, Zhou L, Zhong W and Sheng Y B 2021 *Front. Phys.* **17** 21501
[59] Yan P S, Zhou L, Zhong W and Sheng Y B 2021 *Opt. Express* **29** 9363
[60] Riera-Sàbat F, Sekatski P, Pirker A. and Dür W 2021 *Phys. Rev. A* **104** 012419
[61] Rozpędek F, Schiet T, Thinh L P, Elkouss D, Doherty A C and Wehner S 2018 *Phys. Rev. A* **97** 062333
[62] Krastanov S, Albert V V and Jiang L 2019 *Quantum* **3** 123
[63] Pan J W, Gasparoni S, Ursin R, Weihs G and Zeilinger A 2003 *Nature* **417** 423
[64] Chen L K, Yong H L, Xu P, Yao X C, Xiang T, Li Z D, Liu C, Lu H, Liu N L, Li L, Yang T, Peng C Z, Zhao B, Chen Y A and Pan J W 2017 *Nat. Photonics* **11** 695
[65] Reichle R, Leibfried D, Knill E, Britton J, Blakestad R B, Jost J D, Langer C, Ozeri R, Seidelin S and Wineland D J 2006 *Nature* **443** 838
[66] Hu X M, Huang C X, Sheng Y B, Zhou L, Liu B H, Guo Y, Zhang C, Xing W B, Huang Y F, Li C F and Guo G C 2021 *Phys. Rev. Lett.* **126** 010503
[67] Veldhorst M, Hwang J C C, Yang C H, Leenstra A W, de Ronde B, Dehollain J P, Muhonen J T, Hudson F E, Itoh K M, Morello A and Dzurak A S 2014 *Nat. Nanotechnol.* **9** 981
[68] Pursley B C, Carter S G, Yakes M K, Bracker A S and Gammon D 2018 *Nat. Commun.* **9** 115
[69] Berezovsky J, Mikkelsen M H, Stoltz N G, Coldren L A and Awschalom D D 2008 *Science* **320** 349
[70] Reithmaier J P, Sek G, Löffler A, Hofmann C, Kuhn S, Reitzenstein S, Keldysh L V, Kulakovskii V D, Reinecke T L and Forchel A 2004 *Nature* **432** 197
[71] Abe E, Wu H, Ardavan A and Morton J J L 2011 *Appl. Phys. Lett.* **98** 251108
[72] Lagoudakis K G, Fischer K, Sarmiento T, Majumdar A, Rundquist A, Lu J, Bajcsy M and Vučković J 2013 *New J. Phys.* **15** 113056
[73] Hu C Y, Young A, O'Brien J L, Munro W J and Rarity J G 2008 *Phys. Rev. B* **78** 085307
[74] Soudagar Y, Bussières F, Berlín G, Lacroix S, Fernandez J and Godbout N 2007 *J. Opt. Soc. Am. B* **24** 226
[75] Han X, Hu S, Guo Q, Wang H F and Zhang S 2015 *Quantum Inf. Process.* **14** 1919